Earth Surf. Dynam. Discuss., doi:10.5194/esurf-2016-5, 2016
Manuscript under review for journal Earth Surf. Dynam.
Published: 10 February 2016

Earth Surface Dynamics Discussions
Open Access
EGU

Delineating incised stream sediment sources within a San Francisco Bay tributary basin

Paul Bigelow[1], Lee Benda[2], Sarah Pearce[3]

[1] Bigelow Watershed Geomorphology, Oakland, California, USA
[2] Terrain Works, Mount Shasta, California, USA
[3] San Francisco Estuary Institute, Richmond, California, USA

Correspondence to: Paul Bigelow (paul@bigwatershed.com)

Abstract. Erosion and sedimentation pose ubiquitous problems for land and watershed managers, requiring delineation of sediment sources and sinks across landscapes. However, the technical complexity of many spatially explicit erosion models precludes their use by practitioners. To address this critical gap, we demonstrate a contemporary use of applied geomorphometry through a straightforward GIS analysis of sediment sources in the San Francisco Bay Area in California, USA, designed to support erosion reduction strategies. Using 2 m LiDAR DEMs, we delineated the entire river network in the Arroyo Mocho watershed (573 km^2) at the scale of ~30 m segments and identified incised landforms using a combination of hillslope gradient and planform curvature. Chronic erosion to the channel network was estimated based on these topographic attributes and the density and size of vegetation, and calibrated to sediment gage data, providing a spatially explicit estimate of sediment yield from incised channels across the basin. Rates of erosion were summarized downstream through the channel network, revealing patterns of sediment supply at the reach scale. Erosion and sediment supply were also aggregated to subbasins, allowing comparative analyses at the scale of tributaries. The erosion patterns delineated using this approach provide land use planners with a robust framework to design erosion reduction strategies. More broadly, the study demonstrates a modern analysis of important geomorphic processes affected by land use that is easily applied by agencies to solve common problems in watersheds, improving the integration between science and environmental management.

1 Introduction and Objective

Incised channels are part of a common erosional cycle that pose challenges to watershed management across the globe. Incised channels (inner gorges, arroyos, gullies, ravines, etc.) are often created by headward incision of the channel network in response to local or regional base-level lowering (Schumm et al. 1984) or disturbances that increase sediment transport relative to supply (Schumm 1999), such as land use changes like urbanization that greatly increase runoff (Booth 1991). Characteristically, channel incision continues until a new equilibrium grade is achieved, then the channel widens by eroding oversteepened banks, and aggradation begins (Schumm et al. 1984). In some environments, incised channels are part of a natural alternating cycle of aggradation and degradation in response to episodic sediment supply (Bull 1997). Channel incision creates a variety of problems including destruction of valley bottoms (arable land) and increased sediment yield aggrading downstream reaches (Patton and Schumm 1975, Poesen et al. 2003).

Delineating the extent of channel incision across a watershed or landscape and quantifying erosion from such sources are necessary to design erosion and channel sedimentation abatement measures. Mapping gullies using remote sensing began in the 1970s (e.g., Patton and Schumm 1975) but advancing digital technology in the 21st century now allows for ever more detailed mapping using geographic information systems (GIS) and digital elevation models (DEM). Mapping the extent of incised

Earth Surf. Dynam. Discuss., doi:10.5194/esurf-2016-5, 2016
Manuscript under review for journal Earth Surf. Dynam.
Published: 10 February 2016

channels can involve visual detection in conjunction with delineating a zone around channels based on stream order using GIS (called buffering) (Perroy et al. 2010) or more automated approaches could be applied using digital terrain analysis (Evans and Lindsey 2010, Castillo et al. 2014) or object-oriented classification of gullies (Shruthi et al. 2011, Johansen et al. 2012). Quantifying erosion rates along incised channels often involves calculating the surface elevation difference between current and pre-gully DEMs (Perroy et al. 2010, Evans and Lindsay) or using a time series of DEMs (Martınez-Casasnovas 2003). Spatially distributed estimates of sediment yield from incised channels often require highly parameterized and calibrated models (e.g., Van Rompaey et al. 2001, Pelletier 2012). The technical complexity of such approaches precludes their use by many watershed, land, and resource managers (Guertin and Goodrich 2011) and consequently such agencies often resort to qualitative evaluations or best professional judgment.

In this case study of a San Francisco Bay tributary, we delineate chronic annual erosion from the sides of incised channels and estimate sediment yield at multiple scales using an approach readily understandable and accessible to planners that improves the spatially explicit representation of sediment supply through the channel network. We use a topographic index that combines slope and planform curvature to predict erosion potential (GEP) through the process of shallow failures (Miller and Burnett 2007, Benda et al. 2011). GEP values are calibrated to sediment yield from gage data and then reported to the channel network and aggregated downstresam. In our 'virtual watershed' (Benda et al. 2015, Barquin et al. 2015) we derived a synthetic river network directly from a 2 m LiDAR digital elevation model (DEM) and couple it to the terrestrial landscape via flow direction and accumulation grids. Each ~30 m reach in the virtual watershed is coupled to its local hillslope contributing area (although confined to the incised channel landform in our study application) and GEP and sediment yield values are transferred to the reaches by that contributing area.

The study objective was to delineate and quantify the spatial distribution of chronic sediment supply from incised channels across the Arroyo Mocho watershed in support of erosion reduction strategies. Ultimately, this study demonstrates a straightforward GIS analysis of important geomorphic processes (erosion and sedimentation) often impacted by land use that can be easily applied by watershed and land managers. Within the context of this special issue, our study provides a contemporary example of applied geomorphomety, one designed to increase communication between science and resource planning.

2 Basin Physical Characteristics and Background

Arroyo Mocho basin drains 573 km^2 of the Livermore Valley and is tributary to Arroyo de la Laguna, which joins Alameda Creek and drains to the San Francisco Bay, California (Fig. 1). Basin elevations range between 60 and 1200 m and mean annual precipitation averages 428 mm (Prism 2012). Land use in the watershed includes a mix of urban, residential, and commercial areas concentrated on the Livermore and tributary valley floors, with agriculture (e.g., vineyards) in the lower foothills and rural areas in the uplands. Annual grasses are the dominant vegetation in the watershed. Sparse patches of remaining riparian vegetation in the basin include willows, cottonwoods, occasional oaks, alkali sink scrub, and herbaceous scrub (Stanford et al. 2013), while conifers can be found in the higher elevations. The Livermore Valley is a large tectonically formed depression (pull-apart basin) infilled with late Tertiary and Quaternary alluvial sediment (Graymer et al. 1996, Helley and Graymer 1997). Major tributaries to Arroyo Mocho include Alamo, Tassajara, Cayetano, Altamont, Arroyo Seco, and Las Positas Creeks (Fig. 1). Historically, broad distributary fans formed where these tributaries entered the Livermore Valley floor and lagoon ponding occurred at the western distal end of the valley (Williams 1912), likely in response to massive landsliding from fault rupture

Earth Surf. Dynam. Discuss., doi:10.5194/esurf-2016-5, 2016
Manuscript under review for journal Earth Surf. Dynam.
Published: 10 February 2016

(Ferriz 2001). The fans, valley floor, and marsh were channelized and drained in the late 1800s (Williams 1912) creating a direct conduit to Arroyo de la Laguna (Fig. 1). The region has experienced several cycles of Holocene incision and alluviation from climatic and tectonic forcing and more recently from land use changes and channelization (Rogers 1987, Mero 2015, Williams 1912). Headward growth of stream valleys and canyon cutting (arroyos and gullies) were the dominant geomorphic agents in the basin (Hall 1958), where sediment from these incised channels are now chronically supplied by steep eroding banks (Bigelow et al. 2012a). At larger drainage areas, the incision created continuous arroyos cut into valley fill that are more permanent features on the landscape. At smaller drainage areas, the incision created discontinuous or patchy gullies cut into both narrow valley fills and colluvial hillslopes that are likely more ephemeral features. The engineered flood control channels on the Livermore valley floor (Fig. 1) are currently aggrading in some areas, providing the primary motivation for this study to inform sediment reduction efforts by local government jurisdictions.

In addition to bank erosion from incised channels, mass wasting processes also occur in the uplands, primarily earthflows (Davenport 1985, Wentworth et al. 1997, Roberts et al. 1999, Majmundar 1991 and 1996). The southern hills are underlain by the hard meta-sedimentary rocks of the Cretaceous Franciscan Formation with patchy outcrops of the Plio-Pleistocene Livermore Gravels. Here, the steep topography is dominated by deep-seated landslides or earthflows, most of which are old and no longer active. The eastern hills are underlain by the Cretaceous Great Valley Sequence and Miocene sedimentary units that tend to have steep slopes prone to earthflows. The northern hills are comparatively gentler, underlain by the Livermore Gravels and Miocene sedimentary rocks that produce clay rich soils prone to earthflows.

3 Methods

Channels in the Arroyo Mocho watershed are most often characterized by arroyo or gully forms: an incised topography within a broad valley floor, with steep and occasionally bare eroding banks. The raw banks appear to dominate the chronic annual supply of sediment to channels in the study basin, and thus represent the main source of sediment to the aggrading channels downstream. In general, the low gradient valley floors above arroyo banks cannot topographically erode or deliver sediment to the channel. In the steeper upland channels bordered by colluvial hillslopes (i.e. no valley floor), most of the sediment production occurs on the channel banks and hillslope areas adjacent to the channel, including the toes of earthflows that intersect the channel; hillslopes farther from the channel do not appear to deliver sediment on an annual basis. Based on these observations, we confined the analysis of erosion sources to areas adjacent to channels (e.g., the arroyo or gully landform). We used a GIS buffer of 6 times the bankfull width around the channel that generally captures the steep eroding banks of the incised channel form (e.g., Perroy et al. 2010). To estimate bankfull channel width, we used a San Francisco Bay Area regional regression relationship based on drainage area (Dunne and Leopold 1978). The buffer maximizes the inclusion of hillslope areas that contribute sediment annually (e.g. toes of earthflows), but excludes areas that are not directly connected to channels. The defined erosion source area (98 km^2) is referred to as the buffered incised channel network.

We delineated and quantified the spatial distribution of chronic sediment supply from banks along incised channels that can include earthflow toes (can include the processes of small shallow failures and raveling) across the Arroyo Mocho watershed using a virtual watershed platform (NetMap) that has been applied in similar applications elsewhere (Benda et al. 2007, 2009, 2011, 2015, Bidlack et al. 2014, Barquin et al. 2015, Flitcroft et al. 2015). The primary tasks in the analysis included:

Earth Surf. Dynam. Discuss., doi:10.5194/esurf-2016-5, 2016
Manuscript under review for journal Earth Surf. Dynam.
Published: 10 February 2016

1. Generate a synthetic and attributed stream layer within the virtual watershed.

2. Estimate erosion potential of incised channel banks using a topographic index that includes hillslope gradient and planform curvature.

3. Modify erosion potential based on vegetation density and size.

4. Convert erosion potential to sediment yield using river gage data.

5. Aggregate erosion predictions at various scales: buffered channel reaches, subwatershed, tributary watershed, channel network.

3.1 DEM and Stream Network

An attributed stream channel network was delineated using a 2 m DEM based on algorithms for flow direction and channel delineation described by Clarke et al. (2008). The DEM was compiled and resampled from a 0.3 m DEM for the majority of the watershed within the dominant jurisdictional boundary (Alameda County) and a 3 m DEM for small portions of the watershed that lie in other counties, all derived from Light Detection and Ranging (LiDAR) data collected by the U.S. Geological Survey. The channel network was divided into a linked set of channel segments (ranging from 2 – 80 m length, averaging 30 m). Each segment of the channel network was attributed with a suite of parameters calculated from the DEM including elevation, drainage area, stream gradient, stream order, valley width, and other attributes (Miller et al. 2002, Benda et al. 2007).

3.2 Estimating Erosion Potential from Incised Channels and Other Sources

Erosion in the form of shallow landslides, gullies and surface erosion is often driven by slope steepness and slope curvature (Dietrich and Dunne 1978, Sidle 1987). To estimate a measure of erosion potential in the watersheds, we used a dimensionless index (Eq. 1) that employs slope gradient and local topographic convergence (Miller and Burnett 2007, Benda et al. 2011):

$$GEP = S \cdot a_L/b \quad (1)$$

where GEP is the generic erosion potential, a_L is a measure of local contributing area to a DEM pixel equal to the number of adjacent pixels that drain into it (varies between 0 and 8), and b is a measure of topographic convergence equal to the projection of flow direction out of a pixel onto the pixel edges. Values of b are 1 on planar slopes, less than 1 on convergent topography, and greater than 1 on divergent topography (Miller and Burnett 2007). GEP is a dimensionless index of erosion potential with values from 0 – 1, where larger values correspond to steeper, more convergent topography prone to higher landslide densities, surface erosion, and higher gully-initiation-point densities (Miller and Burnett 2007). Thus, GEP is used as a relative index of erosion potential along the incised channels in the Arroyo Mucho study area.

3.3 Modifying Erosion Potential by Vegetation

We observed that arroyo and gully bank erosion was often reduced by vegetation in the Arroyo Mocho basin, where larger and denser vegetation created stable channel bottoms and banks. Reaches that had little to no vegetation had more exposed, actively eroding banks compared to reaches that had shrubs or trees established on the banks. Where present, the effect of shrubs and

Earth Surf. Dynam. Discuss., doi:10.5194/esurf-2016-5, 2016
Manuscript under review for journal Earth Surf. Dynam.
Published: 10 February 2016

trees in reducing erosion in these arroyo channel systems is particularly pronounced because there is little organic groundcover other than the dominant vegetation of annual grasses. Vegetation reduces erosion by lessening raindrop impact, providing increased soil strength through the root network, and thus reducing surface erosion, rill erosion, and shallow bank slumps and slips (e.g., Thornes 1985, Thorne 1990, Prosser and Dietrich 1995, Simon and Darby 1999, Abernethy and Rutherford 2001, Micheli and Kirchner 2002). In addition, increasing tree age (and thus rooting extent and depth) is related to increasing stability of the soil (Sidle 1987), and tree height and canopy width are proportionally related to rooting width and depth (e.g. McMinn 1963, Smith 1964, Tubbs 1977, Gilman 1988). These relationships provide a basis for using tree height as a proxy for root spread and thus soil stability as described below.

While approaches linking vegetation and associated rooting strength to specific types of erosion have been developed for highly localized scales (e.g., Roering et al. 2003), such empirically-based quantitative approaches to reduce erosion potential using remotely sensed vegetation attributes have yet to be developed. Consequently, many erosion models simply use broad categories of land cover (e.g., forest, scrub, etc.) to reduce erosion potential over vast areas regardless of the individual size of vegetation within the categories (e.g., Renard et al. 1997, Booth et al. 2014) or infer similar generalized relationships, for example, Pelletier (2012) assumed a linear relationship between vegetation (leaf cover) and sediment detachment. We also assume the occurrence of vegetation reduces erosion potential, but use a relationship that includes both the effects of vegetation cover and rooting width and depth in each 2 m grid cell, using tree height as a proxy for root spread and related soil stability. Based on the supporting literature discussed and our field observations that indicate bank erosion activity is related to vegetation density and size (i.e. vegetation height and thus root spread), we developed a simple expression (Eq. 2, Fig. 2) that governs how erosion potential is reduced by vegetation height and use that to scale the GEP index.

$$\text{Erosion reduction} = 0.1906 \ln(\text{tree height in m}) + 0.136 \quad (2)$$

Eq. 2 simulated that grasses are less effective than shrubs, and shrubs are less effective than larger trees in reducing arroyo bank erosion. In the absence of more quantitative techniques, this method provides an incremental improvement on the previous approaches mentioned above. To reduce GEP based on vegetation height, we created a vegetation height and density grid (2 m) in GIS using the first (representing the tallest vegetation) and last (representing the ground surface) return LiDAR points. Because the tree canopy height of each 2 m grid cell is represented, this grid also represents the density of vegetation, another factor that can reduce erosion (e.g. Beeson and Doyle 1995, Wang et al. 2004). We then created an erosion reduction grid by converting (normalizing) the vegetation height grid to the same 0 – 1 scale as GEP where a grid cell with a tree canopy height of 1, 21, or 42 m (maximum tree height) would be normalized to 0 - 1 scale values of 0.14, 0.72, and 0.85, respectively (i.e. 14, 72, and 85% erosion reduction). The resulting erosion reduction grid was subtracted from the initial GEP grid to estimate erosion sources. For example, where a grid cell has a GEP value of 1 and a corresponding erosion reduction value of 0.5, the resulting modified GEP would be 0.5. Where there was no vegetation, GEP values were unchanged. Maximum GEP reduction due to the greatest vegetation height was 0.85 (85%). We were unable to obtain raw LiDAR for Santa Clara County, so it was not possible to create a vegetation reduction grid for this small southeastern portion of the watershed at the headwaters of Arroyo Mocho canyon (Fig. 1).

Earth Surf. Dynam. Discuss., doi:10.5194/esurf-2016-5, 2016
Manuscript under review for journal Earth Surf. Dynam.
Published: 10 February 2016

3.4 Conversion to Sediment Yield

To provide a more meaningful view of spatially explicit erosion across the watershed, we converted the dimensionless GEP index to sediment yield. We linearly scaled the independently estimated sediment yield rate to GEP values. High values of GEP represent higher erosion rates and lower values of GEP represents lower erosion rates. We converted GEP to sediment yield by multiplying each GEP grid cell by the following conversion factor (Eq. 3):

$$\text{conversion factor} = \frac{\text{mean sediment yield rate at Verona Gage}}{\text{mean GEP buffered channel network}} \quad (3)$$

where mean GEP along the buffered channel network is the mean of all GEP grid cells within the buffered channel network (e.g., GMA 2007, Benda 2011). A previous study identified an average sediment yield of 155 tonnes km^{-2} yr^{-1} for the entire drainage area (573 km^2) using sediment collection data from 1994 to 2006 (suspended and bedload) using the Verona Gage on Arroyo de la Laguna (Bigelow et al. 2008)(Fig. 1). In the current application that restricts the analysis to the buffered channel network (drainage area of 98 km^2), an average sediment yield rate of 906 tonnes km^{-2} yr^{-1} was calculated using the same sediment gage data.

3.5 Spatial Distribution of Erosion at Various Scales and through the Channel Network

To evaluate the spatial distribution of chronic sediment sources from incised channels across the study basin, we calculated, aggregated, and mapped GEP and sediment yield at four scales: pixel, buffered reach area, subwatershed, and tributary basin. We also aggregated (summed and area weighted) the estimated sediment yield through the stream network to illustrate how sediment yield varies downstream through the channel network. The aggregated sediment yield value at the bottom of the watershed equals the basin average sediment yield. To estimate sediment eroding to each reach, the buffered channel network was discretized to define the drainage area on each side of the channel reach, also referred to as local contributing area or drainage wings. The total GEP and sediment yield within the drainage wings were attributed to each segment (reach) of the channel network. To estimate the total sediment yield at a given stream segment, GEP and sediment yield was cumulatively added moving downstream and divided by total upstream drainage area of the buffered channel network.

The delineation of erosion from incised channels was checked with direct field observations and through remote sensing, by draping erosion predictions over satellite imagery.

3.6 Sediment Storage Potential

As indicated previously, sediment supply from the incised Arroyo Mocho channel network is aggrading portions of the engineered flood control channels on the Livermore Valley floor. Sediment supply and aggradation of the flood control channels could be reduced by promoting sediment storage at upstream locations, for example by reconnecting channels to floodplains. To help land managers identify ideal upstream locations for sediment storage, we developed a sediment storage potential index (Eq. 4):

$$\text{storage potential index} = \frac{\text{valley width index}}{\text{stream power index}} \quad (4)$$

Earth Surf. Dynam. Discuss., doi:10.5194/esurf-2016-5, 2016
Manuscript under review for journal Earth Surf. Dynam.
Published: 10 February 2016

where the stream power index is drainage area * gradient, and the valley width index (e.g. Grant and Swanson 1995) is valley width (at 2 x bankfull depth) divided by channel width. Channel width and bankfull depth were estimated using regional regressions (Dunne and Leopold 1978), while gradient, drainage area, and valley width were extracted from the DEM using algorithms within NetMap (Miller et al. 2002, Benda et al. 2007). Stream power reflects the ability of a channel to transport or store sediment, where streams with higher stream power have less opportunity to create large in-channel storage reservoirs in contrast with streams of lower power that can store sediment. The valley width index reflects the potential width of the flood plain for sediment storage.

4 Results and Discussion

4.1 Field and Remote Sensing Observations of Erosion

Viewing roughly 50% of the channel network on satellite imagery, we consistently observed steep eroding banks (bare of vegetation) in areas with high GEP values throughout the watershed. Conversely, we observed much more stable banks with vegetation in areas with lower GEP values. Similar observations were made for earthflow toes. The agreement between erosion predictions and imagery observations was also confirmed during two days of field observations throughout the watershed (Table 1, Fig. 3, also see extensive photo documentation in Bigelow et al. 2012a).

4.2 What is the spatial distribution of chronic erosion from incised channels at various scales across the watershed?

The spatial distribution of erosion (GEP) and sediment yield reveals strong patterns at the scales of pixel, reach, subwatershed, and tributary watershed scales. Starting at the smallest scales, the spatial distribution of GEP and estimated sediment yield can be evaluated at the level of individual pixels (4 m^2) to identify discrete eroding banks (Fig. 3). To place the example shown on Fig. 3 in practical terms for land managers, the eroding bends shown are chronically contributing an estimated 10 tonnes of bank material per year, a little less than one dump truck worth of sediment. This estimate reflects a temporally averaged yield, however, erosion in the region is highly episodic (e.g., Ellen and Wieczorek 1982, Bigelow et al. 2008). Consequently, the actual temporal dynamics are that such a bank may retreat several meters in an extreme event yielding hundreds of tonnes to the channel, followed by many years of little or no erosion. Moving up to the buffered stream reach scale (mean 586 m^2), the spatial distribution of erosion can be used to highlight eroding bends and banks along entire valley segments (Fig. 3).

Scaling up to the subwatershed distribution of erosion (mean 2.7 km^2, Fig. 4) shows the most erosive valley segments are not isolated to a single larger basin, but are generally grouped into several steep or heavily incised areas across the entire Arroyo Mocho watershed. Such areas include steeper uplands or canyon areas where the channel impinges on and erodes high terraces, or where the toes of earthflows impinge on the channel. In addition to these steep erosive subwatersheds, other subwatersheds in the lower Tassajara and Cayetano basins also display higher estimated sediment yields (Fig. 4). These areas are prone to earthflows from clay rich expansive soils produced from the underlying Plio/Pleistocene and Miocene sedimentary units. At the subwatershed scale, the more erosive areas have estimated sediment yields roughly 3 – 8 fold higher than more stable areas (Fig. 4).

The spatial distribution of GEP and estimated sediment yield at the tributary basin scale (mean 51 km^2) varies considerably (Fig. 5). At this largest scale, the more erosive areas are concentrated in the steeper dissected basins of the southeastern and eastern

Earth Surf. Dynam. Discuss., doi:10.5194/esurf-2016-5, 2016
Manuscript under review for journal Earth Surf. Dynam.
Published: 10 February 2016

watershed, primarily the upper Arroyo Mocho basins, Arroyo Seco, and Altamont Creek, where GEP values and estimated sediment yield are 3 fold higher than western areas at the basin scale (Fig. 5).

4.3 What is the estimated sediment yield down through the channel network?

Estimated sediment yields aggregated through the stream network (summed and area weighted) illustrate how sediment yield varies downstream through the channel network (Fig. 6). Similar to the spatially explicit distribution of GEP and sediment yield across the terrain (Figs. 3 - 5), this channel segment scale analysis illustrates higher sediment supply from the more dissected steep terrain of Arroyo Mocho canyon. We also aggregated the total sediment yield downstream by segment and divided it by the total load to show the percentage of the load by tributary (Fig. 7).

4.4 How Can Spatially Explicit Erosion Estimates Inform Sediment Reduction Efforts?

Prioritize sediment source control. The spatial distribution of GEP and estimated sediment yield at the various scales across the terrain and through the channel network provides a physical basis for evaluating and prioritizing sediment reduction strategies within a large watershed or region. The spatial distribution of erosion at the subwatershed scale (Fig. 4) is perhaps the most useful for prioritizing potential source control activities, where as the spatial distribution of sediment yield through the channel network (Fig. 6) can focus source control at a finer scale, showing which channels to focus on, rather than entire subwatersheds. This spatially explicit representation of erosion allows watershed managers to target limited funds to areas where they will achieve the most reduction in sediment supply.

Prioritize areas for sediment storage. In combination with the spatial distribution of erosion (Figs. 3 – 7), watershed managers can also use other parameters extracted from the DEM to prioritize areas for sediment storage downstream of the most erosive areas. In our study basin, the Livermore Valley was historically highly depositional, where tributaries deposited sediment as broad coalescing fans across the valley floor (Williams 1912). Where there is sufficient space to allow channels to reoccupy floodplains, we estimated ideal locations for promoting sediment storage (e.g., reconnection of channels to floodplains). Using Eq. 4, sediment storage potential is estimated to vary considerably across the stream network, where certain portions of the mainstem streams are estimated to have a higher potential for sediment storage compared to other segments (Fig. 8). These estimations do not capture local forcing of sediment storage from channel constrictions (e.g. bridges) or tributary confluences that may exert primary controls on aggradation.

5 Utility and Adjustments

The spatially explicit erosion modeling approach used here demonstrates a straightforward GIS analysis incorporating contemporary geomorphmetric techniques that only requires a DEM and vegetation height layer and characterizes erosion from incised stream banks and the toes of earthflows. The erosion model can also be used to characterize most other forms of erosion (e.g., Miller and Burnett 2007, Benda et al. 2011). Accordingly, this approach should appeal to those seeking a simpler easily applied erosion model with wider applications compared to more complex models that are highly parameterized or limited to specific erosion processes. Like all geospatial tools and models, this approach can be adapted and improved for specific applications and objectives. For instance, erosion rates could be adjusted based on other factors not accounted for in this study such as higher erosion rates for weaker lithologies or precipitation gradients across large basins. As an example, we describe two

Earth Surf. Dynam. Discuss., doi:10.5194/esurf-2016-5, 2016
Manuscript under review for journal Earth Surf. Dynam.
Published: 10 February 2016

potential improvements to refine estimates in our study basin to characterize longer term, decadal sediment yield and the bedload component.

Decadal Sediment Supply. The estimated sediment yield in this study represents an average condition using only topographic and vegetation attributes that characterize chronic (annual or persistent) sediment supply from bare steep channels banks. However, sediment supply in many landscapes is highly variable in both space and time resulting from episodic processes driven by interactions among storms, vegetation, and topography (Benda and Dunne 1997). In the San Francisco Bay region, episodic mass wasting triggered during El Niño storms can dominate decadal sediment supply (Ellen and Wieczorek 1982, Bigelow et al. 2008). For example, Arroyo Mocho is tributary to Alameda Creek, where a single flood event comprised 48% of the total load over a 13-year period (Brown and Jackson 1973). Episodic mass wasting sources in decadal sediment supply can be estimated through a more detailed sediment budget approach (e.g., Reid and Dunne 1996), or more simply by increasing the sediment yield in active mass wasting areas based on regional literature values. For example, two similar studies (GMA 2007, Bigelow et al. 2012b) used digitized maps of active earthflows and local literature values of earthflow rates to appropriately increase the sediment yield estimates at these discrete locations within the watersheds. This approach in part accounts for differences in lithologic erosion rates across the basin, as higher sediment yields from earthflows often occur in specific formations that produce clay rich soils (e.g. Keefer and Johnson 1983).

Bedload Yield. This study approach characterizes total sediment supply to the stream network without regard to the proportion of bedload to the overall yield. Some characterization of the bedload yield variation throughout the stream network would better constrain source control efforts to areas that have a higher bedload yield aggrading downstream reaches. Primary controls on bedload yield are typically drainage area and lithology, where the proportion of bedload generally decreases downstream due to particle attrition (abrasion and breakage) (e.g. Madej 1995, Benda and Dunne 1998) and attrition rates will also vary based on lithology, where harder rocks in a catchment produce a larger bedload component (Madej 1995, Turowski et al. 2012, Mueller and Pitlick 2013, O'Connor et al. 2014). This type of characterization could involve tumbling mill analysis of colluvium throughout the watershed to estimate attrition rates by lithology (e.g., O'Connor et al. 2014). The spatially variable bedload yield throughout the stream network could be simply estimated by a proportion of the overall sediment yield that decreases exponentially with increasing drainage area (e.g., Dietrich and Dunne 1978). This decay function would be further adjusted based directly on lithology attrition rates within the watershed relative to each other. More involved estimates of the variation in bedload yield are also possible (e.g., Madej 1995, Collins and Dunne 1989, Benda and Dunne 1997).

Acknowledgements. The Zone 7 Water Agency funded an initial study that provided the basis for this manuscript. Jamie Kass and Julie Beagle helped obtain and process the LiDAR data and develop the vegetation height grid. Kevin Andras developed the NetMap GIS layers. Lester McKee provided a review of the initial study report. We thank all of these people for their support of this project. The three coauthors donated their time to prepare this manuscript. We also express our sincere gratitude to David Bowie, for his beautiful and inspiring life and music that make "the stars look very different today".

References

Abernethy, B., and Rutherford, I. D.: The distribution and strength of riparian tree roots in relation to riverbank reinforcement, Hydrol. Process., 15, 63–79, 2001.

Barquín, J., Benda, L. E., Villa, F., Brown, L. E., Bonada, N., Vieites, D. R., Battin, T. J., Olden, J. D., Hughes, S. J., Gray, C. and Woodward, G.: Coupling virtual watersheds with ecosystem services assessment: a 21st century platform to support river research and management, WIREs Water, doi:10.1002/wat2.1106, 2015.

Beeson, C. E., and Doyle, P. E.: Comparison of bank erosion at vegetated and non-vegetated channel bends. Water Resour. Bull., 31, 983-990, 1995.

Benda, L., and Dunne, T.: Stochastic forcing of sediment routing and storage in channel networks, Water Resour. Res., 33, 2865-2880, 1997.

Benda, L., Miller, D. J., Andras, K., Bigelow, P., Reeves, G., and Michael, D.: NetMap: a new tool in support of watershed science and resource management, Forest Sci., 52, 206–219, 2007.

Benda, L., Miller, D., and Barquín, J. 2011. Creating a catchment perspective for river restoration, Hydrol. Earth Syst. Sci. Discuss., 8, 2929-2973, doi:10.5194/hessd-8-2929-2011.

Benda, L., Miller, D., Barquin, J., McCleary, R., Cai, T., and Ji, Y.: Building virtual watersheds: a global opportunity to strengthen resource management and conservation, Environ. Manage., 1-18, 2015.

Bidlack, A. L., Benda, L. E., Miewald, T., Reeves, G. H., & McMahan, G.: Identifying suitable habitat for chinook salmon across a large, glaciated watershed, T. Am. Fish. Soc., 143, 689-699, 2014.

Bigelow, P., Pearce, S., McKee, L., and Gilbreath, A.: A sediment budget for two reaches of Alameda Creek, prepared for the Alameda Flood Control and Water Conservation District, 144 pp., 2008.

Bigelow P., Benda, L., Pearce, S., Andras, K., Beagle, J., Kass, J., and McKee, L.: Relative erosion estimates for Arroyo Mocho Watershed using GIS-based terrain mapping, prepared for the Zone 7 Water Agency, 33 pp., 2012a.

Bigelow, P., Pearce, S., and McKee, L.: Evaluation of Sediment Sources to Don Castro Reservoir: on the magnitude, spatial distribution, and potential reduction of sediment supply in the Upper San Lorenzo Creek watershed, prepared for the Alameda County Flood Control and Water Conservation District, 47 pp., 2012b.

Booth, D. B.: Urbanization and the natural drainage system--impacts, solutions, and prognoses, the Northwest Environmental Journal, 7, 91-118, 1991.

Booth, D. B., Leverich, G., Downs, P. W., Dusterhoff, S., and Araya, S.: A method for spatially explicit representation of sub-watershed sediment yield, southern California, USA, Environmental management, *53*, 968-984, 2014.

Brown, W. M., and Jackson, L. E.: Erosional and depositional provinces and sediment-transport in the south central San Francisco Bay region, California, U.S. Geological Survey, Miscellaneous Field Studies Map 515, 1973.

Bull, W. B.: Discontinuous ephemeral streams, Geomorphology, 19, 227-276, 1997.

Castillo, C., Taguas, E. V., Zarco-Tejada, P., James, M. R., & Gómez, J. A.: The normalized topographic method: an automated procedure for gully mapping using GIS, Earth Surf. Proc. Land., 39, 2014.

Clarke, S., Burnett, K. M., and Miller, D. J.: Modeling streams and hydrogeomorphic attributes in Oregon from digital and field data, J. Am. Water Resour. Assoc., 44, 459–477, 2008.

Collins, B., and Dunne, T.: Gravel transport, gravel harvesting and channel-bed degradation in rivers draining the southern Olympic Mountains, Washington, U.S.A., Environ. Geol. 13, 213-224, 1989.

Davenport, C. W.: Landslide hazards in parts of the Diablo and Dublin 7.5' quadrangles, Contra Costa County, California, California Division of Mines and Geology Open-File Report 86- 7 SF, Landslide Hazard Identification Map No. 3, 1985.

Dietrich, W. E. and Dunne, T.:L Sediment Budget for a Small Catchment in Mountainous Terrain: Zietschrift fur Geomorphologie, Suppl., 29, 191-206, 1978.

Dunne, T., and Leopold L. B.: Water in environmental planning, W. H. Freeman & Company, San Francisco, 818 pp., 1978.

Earth Surf. Dynam. Discuss., doi:10.5194/esurf-2016-5, 2016
Manuscript under review for journal Earth Surf. Dynam.
Published: 10 February 2016

Ellen, S. and Wieczorek, G. F. (Eds): Landslides, floods, and marine effects of the storm of January 3-5, 1982, in the San Francisco Bay region, California, U. S. Geological Survey Professional Paper 1434, 319 pp., 1988.

Evans, M., and Lindsay, J.: Quantifying gully erosion in upland peatlands at the landscape scale, Earth Surf. Proc. Land., 35, 876–886, 2010.

Ferriz, H.: Groundwater resources of northern California: an overview. Engineering geology practice in northern California Bulletin, 210, 19-47, 2001.

Flitcroft, R. L., Falke, J. A., Reeves, G. H., Hessburg, P. F., McNyset, K. M. and Benda, L. E.: Wildfire may increase habitat quality for spring Chinook salmon in the Wenatchee River subbasin, WA, USA, Forest Ecol. Manag., 359, 126-140, 2016.

Gilman, E.: Predicting root spread from trunk diameter and branch spread. Journal of Arboriculture, 14, 85–89, 1988.

GMA: Mad River total maximum daily loads for sediment and turbidity: appendix a: sediment source analysis, prepared for the U.S. EPA by Graham Matthews & Associates, 173 pp., 2007.

Grant, G. E., and Swanson, F. J.: Morphology and processes of valley floors in mountain streams, western Cascades, Oregon, Natural and anthropogenic influences in fluvial geomorphology, Geophysical Monograph – American Geophysical Union, 89, pp. 83–101, 1995.

Graymer, R. W., Jones, D. L., and Brabb, E. E.: Preliminary geologic map emphasizing bedrock formations in Alameda County, California: a digital database, U.S. Geological Survey Open-File Report 96-252, 1996.

Guertin, D. P., and Goodrich, D. C.: The future role of information technology in erosion modeling, In Handbook of erosion modeling, Morgan, R. P. C., and Nearing, M. Eds., John Wiley & Sons, 324 - 338, 2011.

Hall, C. A.: Geology and paleontology of the Pleasanton area, Alameda and Contra Costa counties, California, University of California Press, 89 pp., 1958.

Helley, E. J., and Graymer, R. W.: Quaternary geology of Alameda County, and parts of Contra Costa, Santa Clara, San Mateo, San Francisco, Stanislaus, and San Joaquin Counties, California: a digital database, U.S. Geological Survey Open-File Report: 97-97, 1997.

Johansen, K., Taihei, S., Tindall, D., and Phinn, S.: Object-based monitoring of gully extent and volume in north Australia using LiDAR data, Proceedings of the 4th GEOBIA, May 7-9, 2012.

Keefer, D. K., and Johnson, A. M.: Earth flows – morphology, mobilization and movement, U.S. Geological Survey Professional Paper 1264, 56 pp., 1983.

Madej, M. A.: Changes in channel-stored sediment, Redwood Creek, Northwestern California, 1947-1980, Chapter O in U.S. Geological Survey Professional Paper 1454, Geomorphic processes and aquatic habitat in the Redwood Creek basin, Northwestern California. Nolan, K. M., Kelsey, H. M., and Marron, D. C. (Eds.), 1995.

Martınez-Casasnovas, J. A.: A spatial information technology approach for the mapping and quantification of gully erosion, Catena, 50, 293-308, 2003.

Majmundar, H. H.: Landslide hazards in the Livermore Valley and vicinity, Alameda and Contra Costa Counties, California, Calif. Div. Mines and Geology Open-file Report 91-02, Landslide Hazard Identification Map 21, 1991.

Majmundar, H. H.: Landslides and related features, in Landslide hazards in the Hayward quadrangle and parts of the Dublin quadrangle, Alameda and Contra Costa Counties, California: Calif. Div. Mines and Geology, Open-file Report 95-14, plate B, 1996.

McMinn, R. G.: Characteristics of Douglas-fir root systems, Canadian Journal of Botany, 41, 105–122, 1963.

Mero, W. E.: Megaflood and Megadrought - How They Changed Contra Costa, Contra Costa County Historical Society, available at http://www.cocohistory.org/essays-megaflood.html, 2015.

Micheli, E. R., and Kirchner, J. W.: Effects of wet meadow riparian vegetation on streambank erosion. 2. Measurements of vegetated bank strength and consequences for failure mechanics, Earth Surf. Process. Landforms, 27, 687–697, doi: 10.1002/esp.340, 2002.

Miller, D., Benda, L., Furniss, M., and Penney, M.: Program for DEM analysis, in Landscape Dynamics and Forest Management. Gen. Tech. Rep. RMRS-GTR-101CD, U.S. Forest Service, Rocky Mountain Research Station, Fort Collins, CD-ROM, 2002.

Miller, D. J., and Burnett, K. M. Effects of forest cover, topography, and sampling extent on the measured density of shallow, translational landslides, Water Resour. Res., 43, 1–23, 2007.

Mueller, E. R., and Pitlick, J.: Sediment supply and channel morphology in mountain river systems: 1. Relative importance of lithology, topography, and climate, J. Geophys. Res. Earth Surf., 118, 2325–2342, doi:10.1002/2013JF002843, 2013.

O'Connor, J. E., Mangano, J. F., Anderson, S. W., Wallick, J. R., Jones, K. L., and Keith, M. K.: Geologic and physiographic controls on bed-material yield, transport, and channel morphology for alluvial and bedrock rivers, western Oregon, Geol. Soc. Am. Bull., 126, 377–397; doi:10.1130/B30831.1, 2014.

Patton, P. C., and Schumm, S. A.: Gully erosion, Northwestern Colorado: a threshold phenomenon, Geology, 3, 88-90, 1975.

Pelletier, J. D.: A spatially distributed model for the long-term suspended sediment discharge and delivery ratio of drainage basins, J. Geophys. Res., 117, doi:10.1029/2011JF002129, 2012.

Perroy, R. L., Bookhagen, B., Anser, G. P., and Chadwick, O. A.: Comparison of gully erosion estimates using airborne and ground-based LiDAR on Santa Cruz Island, California, Geomorphology, 118, 288–300, 2010.

Poesen, J., Nachtergaele, J., Verstraeten, G., and Valentin, C.: Gully erosion and environmental change: importance and research needs. Catena, 50, 91-133, 2003.

Prism: Oregon State University parameter-elevation regressions on independent slopes model (Prism) climate mapping system and climate data archive, available at http://www.prism.oregonstate.edu, 2012.

Prosser, I. P., and Dietrich, W. E.: Field experiments on erosion by overland flow and their implication for a digital terrain model of channel initiation, Water Resources Research, 31, 2867-2876, 1995.

Reid, L. M. and Dunne, T.: Rapid evaluation of Sediment Budgets, Catena Verlag, Germany, 164 pp., 1996.

Renard, K. G., Foster, G. R, Weesies, G. A., and McCool, D. K.: Predicting soil erosion by water: a guide planning with the Revised Universal Soil Loss Equation (RUSLE), Agriculture Handbook No. 703, USDA-ARS, 1997.

Rogers, J. D.: Pleistocene to Holocene transition in central Contra Costa County, in: Field trip guide to the geology of the San Ramon Valley and environs, Ron Crane (Ed.), Northern California Geological Society, 29-51, 1988.

Roberts, S., Roberts, M. A., and. Brennan, E.M.: Landslides in Alameda County, California, a digital database extracted from preliminary photointerpretation maps of surficial deposits by T.H. Nilsen in U.S. Geological Survey Open-File Report 75-277, 1999.

Roering, J. J., Schmidt, K. M., Stock, J. D., Dietrich, W. E., and Montgomery, D. R.: Shallow landsliding, root reinforcement, and the spatial distribution of trees in the Oregon Coast Range, Canadian Geotechnical Journal, 40, 237-253, 2003.

Schumm, S. A.: Causes and controls of channel incision, in: Incised river channels: processes, forms, engineering and management, Darby, S. E., and Simon, A. (Eds.), John Wiley and Sons: London, 19-33, 1999.

Schumm, S., Harvey, M., and Watson, C.: Incised channels: morphology, dynamics and control, Water Resource Publication, Littleton, Colorado, 200 pp., 1984.

Shruthi, R. B., Kerle, N., and Jetten, V.: Object-based gully feature extraction using high spatial resolution imagery, Geomorphology, 134, 260-268, 2011.

Earth Surf. Dynam. Discuss., doi:10.5194/esurf-2016-5, 2016
Manuscript under review for journal Earth Surf. Dynam.
Published: 10 February 2016

Sidle, R. C.: A dynamic model of slope stability in zero-order basins, International Association of Hydrological Sciences, Publication 165, 101-110, 1987.

Simon, A., and Darby, S. E.: The nature and significance of incised river channels, in: Incised river channels: processes, forms, engineering and management, Darby S. E, and Simon, A. (Eds.), John Wiley and Sons: London, 3–18, 1999.

Smith, J. G.: Root spread can be estimated from crown width of Douglas Fir, Lodgepole Pine, and other British Columbia tree species, The Forestry Chronicle, 40, 456-473, 1964.

Stanford, B., Grossinger, R. M., Beagle, J., Askevold, R. A., Leidy, R. A., Beller, E. E., Salomon, M., Striplen, C. J., and Whipple, A.: Alameda Creek watershed historical ecology study. Richmond, California, San Francisco Estuary Institute-Aquatic Science Center, 2013.

Thorne, C. R.: Effects of vegetation on riverbank erosion and stability, in: Vegetation and erosion: processes and environments, Thornes, J. B. (ed.), John Wiley and Sons, Chichester, United Kingdom, 125–144, 1990.

Thornes, J. B.: The ecology of erosion, Geography, 70, 222-235, 1985.

Tubbs, C. H.: Root-crown relations of young sugar maple and yellow birch, Research Note NC-225, U.S. Forest Service, North Central Forest Experiment Station, 4 pp., 1977.

Van Rompaey, A., Verstraeten, G., Van Oost, K., Govers, G., and Poesen, J. Modelling mean annual sediment yield using a distributed approach, Earth Surf. Proc. Land., 26, 1221-1236, 2001.

Wang, Z. Y., Huang, G. H., Wang, G. Q., and Gao, J.: Modeling of vegetation-erosion dynamics in watershed systems, J. Environ. Eng.-ASCE., 130, 792-800, 2004.

Wentworth, C. M., Graham, S. E., Pike, R. I., Beukelman, G. S., Ramsey, D. W., and Barron, A. D.: Summary distribution of slides and earth flows in Alameda County, California, U.S. Geological Survey OF 97-745, 1997.

Williams, C.: Report on the water supply of the Alameda Creek watershed, with particular reference to the Livermore Valley underground supply: City of San Francisco, 1912.

Earth Surf. Dynam. Discuss., doi:10.5194/esurf-2016-5, 2016
Manuscript under review for journal Earth Surf. Dynam.
Published: 10 February 2016

Earth Surface Dynamics Discussions
Open Access
EGU

Table 1. Summary of agreement between erosion (GEP) predictions and erosion observed on satellite imagery and in the field.

Tributary Basin	GEP Value	Observed
Lower Alamo Creek	High	High
Lower Alamo Creek	Moderate	Moderate
Lower Alamo Creek	Low	Low
Upper Alamo Creek	High	High
Upper Alamo Creek	Moderate	Moderate
Upper Alamo Creek	Low	Low
Lower Tassajara Creek	High	High
Lower Tassajara Creek	Moderate	Moderate
Lower Tassajara Creek	Low	Low
Upper Tassajara Creek	High	High
Upper Tassajara Creek	Moderate	Moderate
Upper Tassajara Creek	Low	Low
Cayetano Creek	High	High
Cayetano Creek	Moderate	Moderate
Cayetano Creek	Low	Low
Altamont Creek	High	High
Altamont Creek	Moderate	Moderate
Altamont Creek	Low	Low
Arroyo Seco	High	High
Arroyo Seco	Moderate	Moderate
Arroyo Seco	Low	Low
Lower Arroyo Mocho	High	High
Lower Arroyo Mocho	Moderate	Moderate
Lower Arroyo Mocho	Low	Low
Middle Arroyo Mocho	High	High
Middle Arroyo Mocho	Moderate	Moderate
Middle Arroyo Mocho	Low	Low
Upper Arroyo Mocho	High	High
Upper Arroyo Mocho	Moderate	Moderate
Upper Arroyo Mocho	Low	Low
Top Arroyo Mocho	High	High
Top Arroyo Mocho	Moderate	Moderate
Top Arroyo Mocho	Low	Low

Earth Surf. Dynam. Discuss., doi:10.5194/esurf-2016-5, 2016
Manuscript under review for journal Earth Surf. Dynam.
Published: 10 February 2016

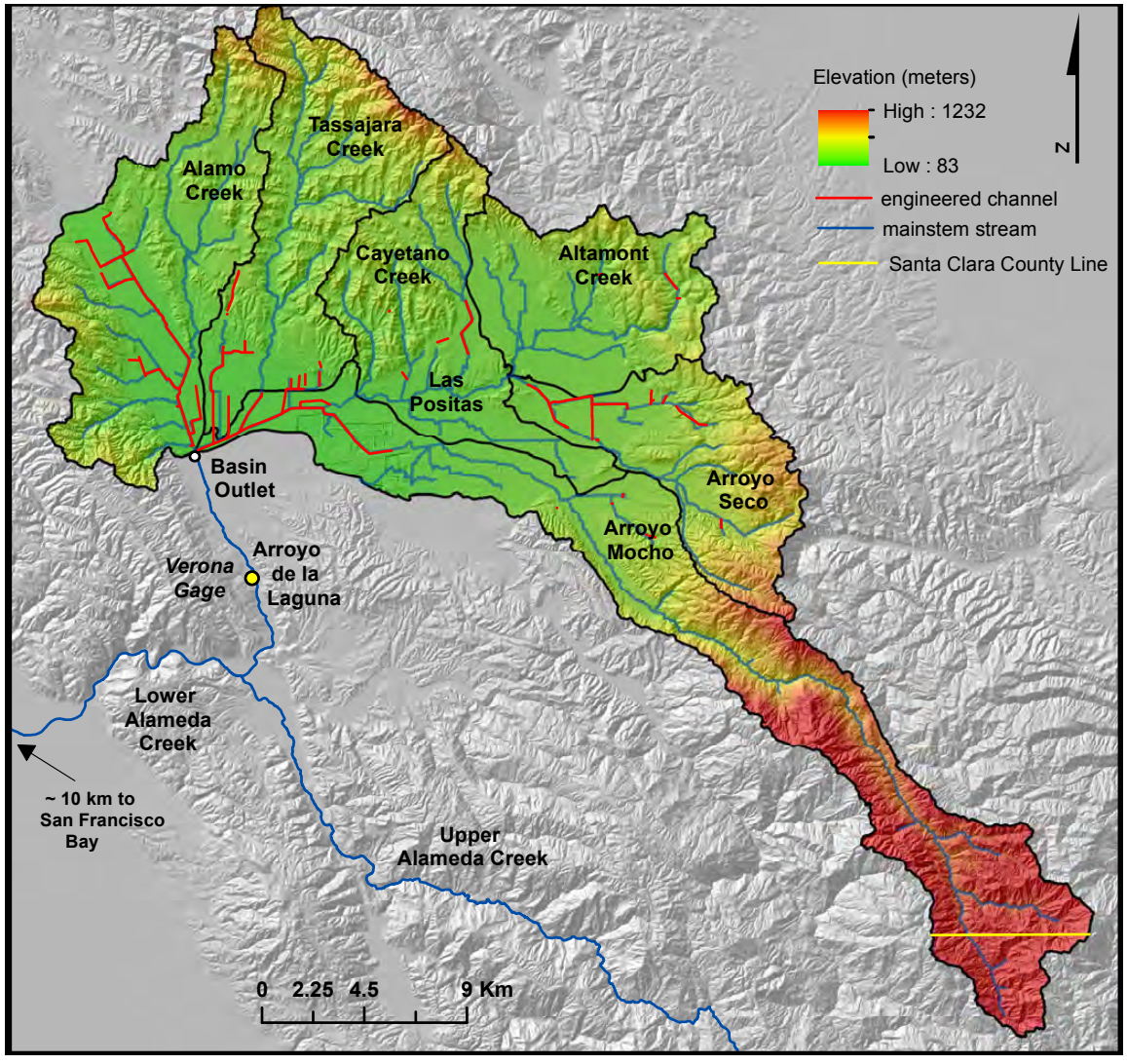

Figure 1. Arroyo Mocho watershed showing the six major basins, mainstem channels, and flood control channels.

Earth Surf. Dynam. Discuss., doi:10.5194/esurf-2016-5, 2016
Manuscript under review for journal Earth Surf. Dynam.
Published: 10 February 2016

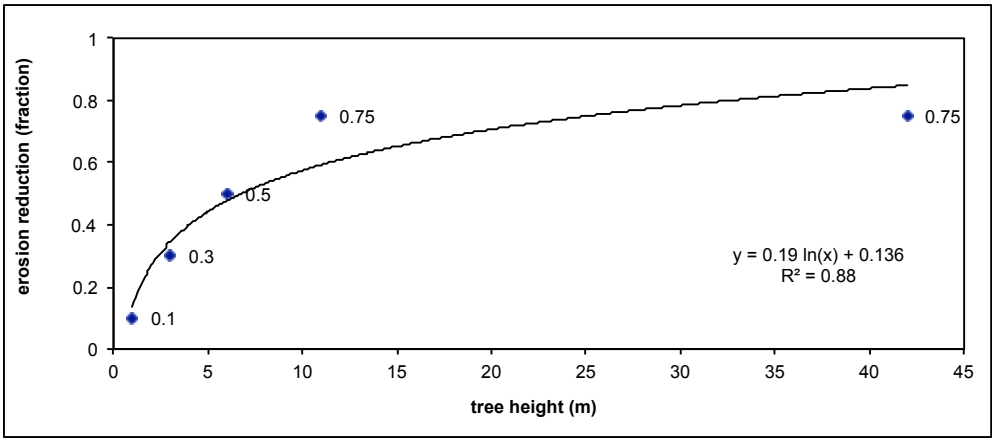

Figure 2. Estimated general relationship between tree height (as a proxy for root spread) and erosion reduction (bank stability) used to scale GEP estimates. Relationship based on field observations and the general relationship between vegetation size and bank stability (see text for details).

Earth Surf. Dynam. Discuss., doi:10.5194/esurf-2016-5, 2016
Manuscript under review for journal Earth Surf. Dynam.
Published: 10 February 2016

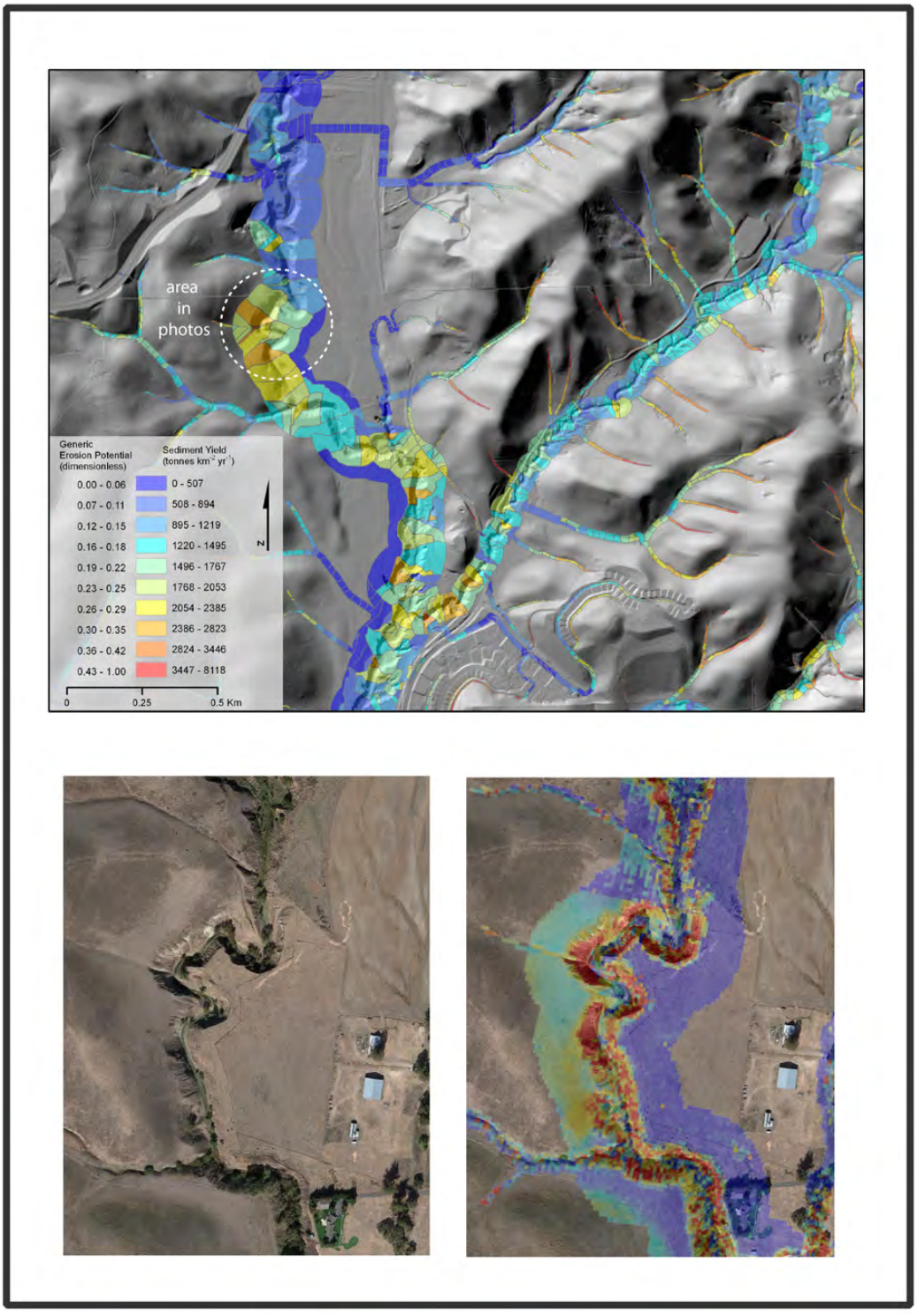

Figure 3. Incised channel on lower Tassajara Creek basin showing GEP and estimated sediment yield at the reach scale (upper) and satellite image (lower left) with pixel scale GEP draped over image (lower right).

Earth Surf. Dynam. Discuss., doi:10.5194/esurf-2016-5, 2016
Manuscript under review for journal Earth Surf. Dynam.
Published: 10 February 2016

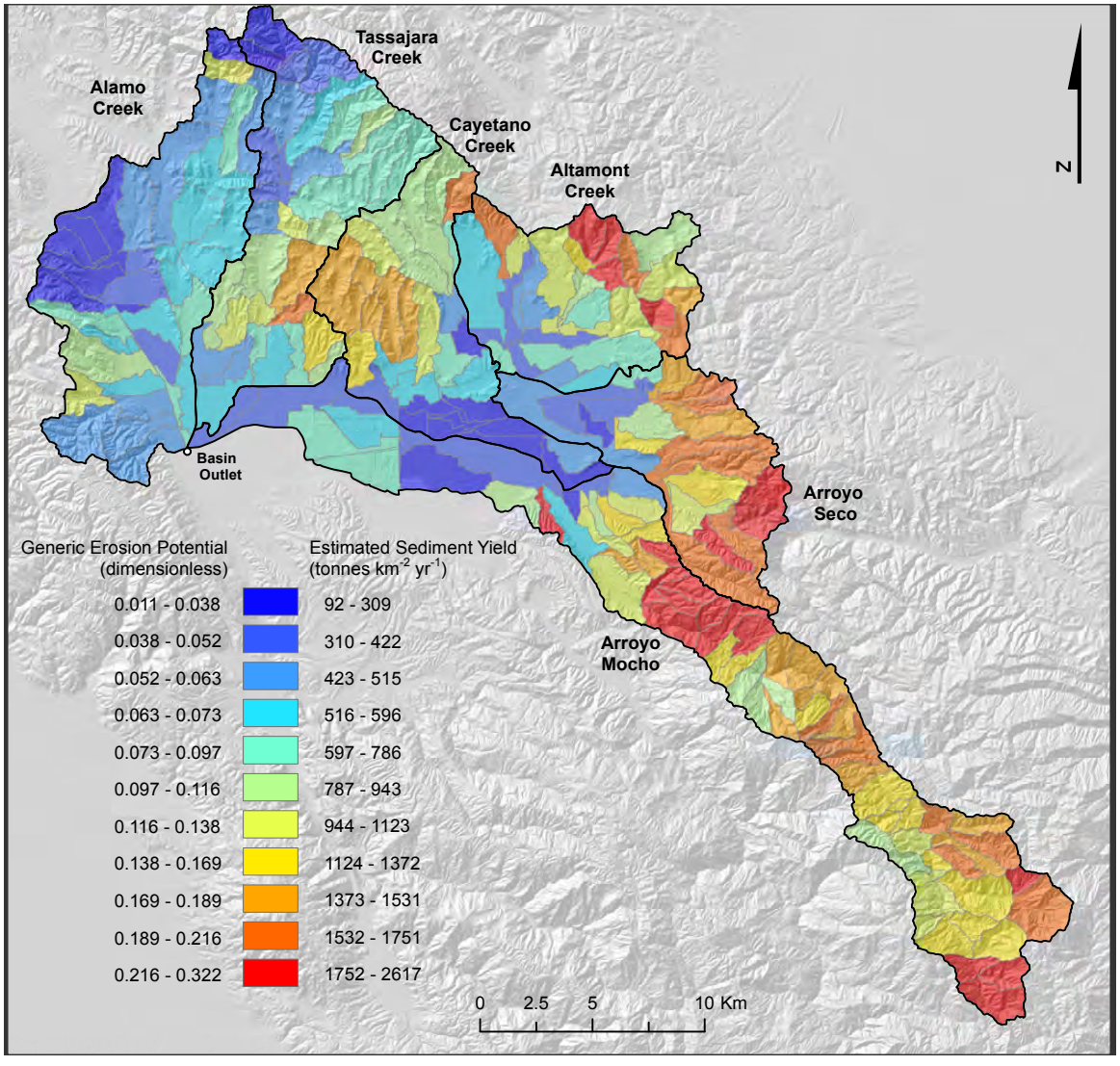

Figure 4. GEP and estimated sediment yields at the subwatershed scale.

Earth Surf. Dynam. Discuss., doi:10.5194/esurf-2016-5, 2016
Manuscript under review for journal Earth Surf. Dynam.
Published: 10 February 2016

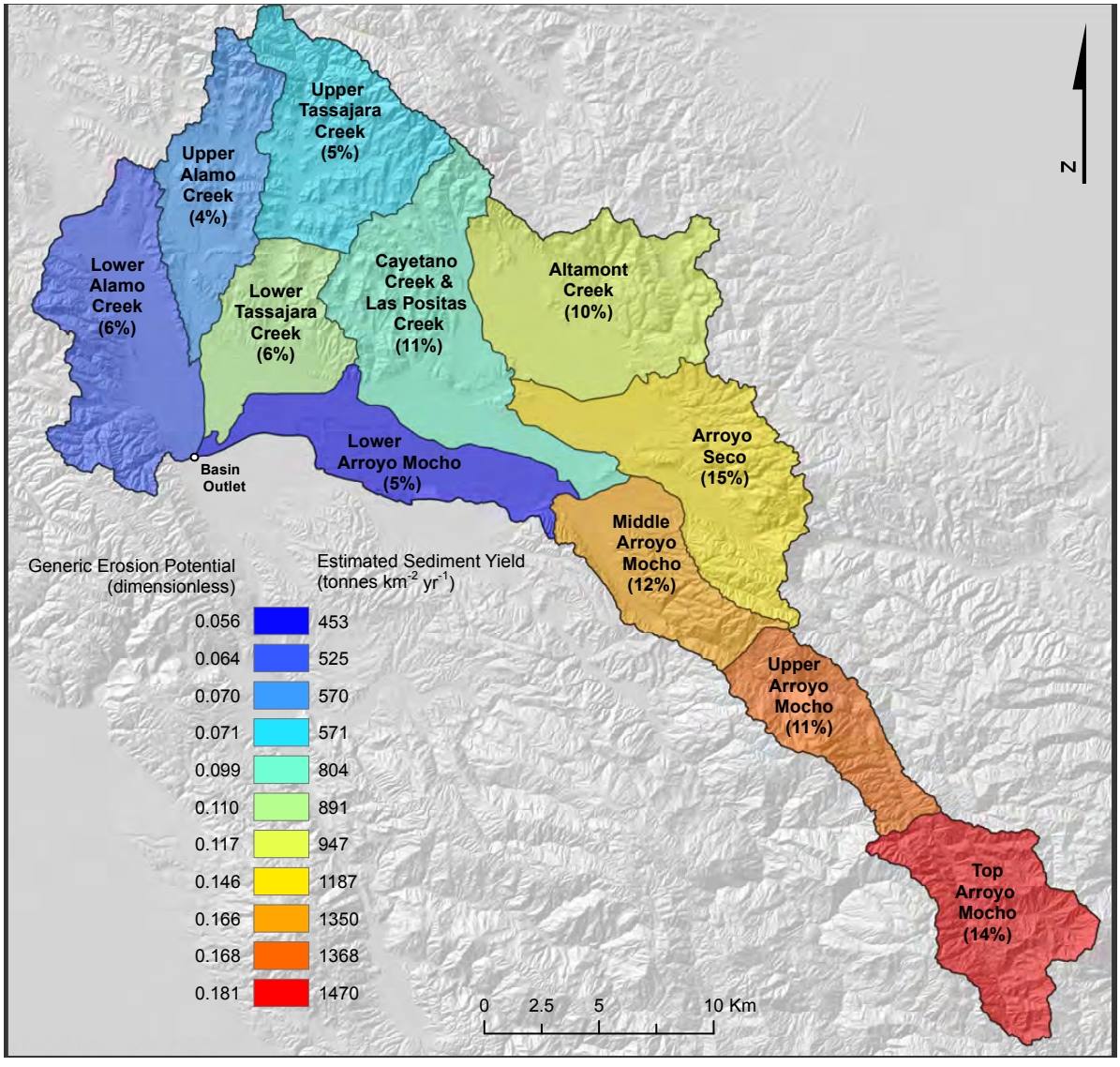

Figure 5. GEP and estimated sediment yields for the 11 major basins in the Arroyo Mocho watershed. Values in parentheses are the percentage of the total estimated sediment yield for Arroyo Mocho contributed by each basin.

Earth Surf. Dynam. Discuss., doi:10.5194/esurf-2016-5, 2016
Manuscript under review for journal Earth Surf. Dynam.
Published: 10 February 2016

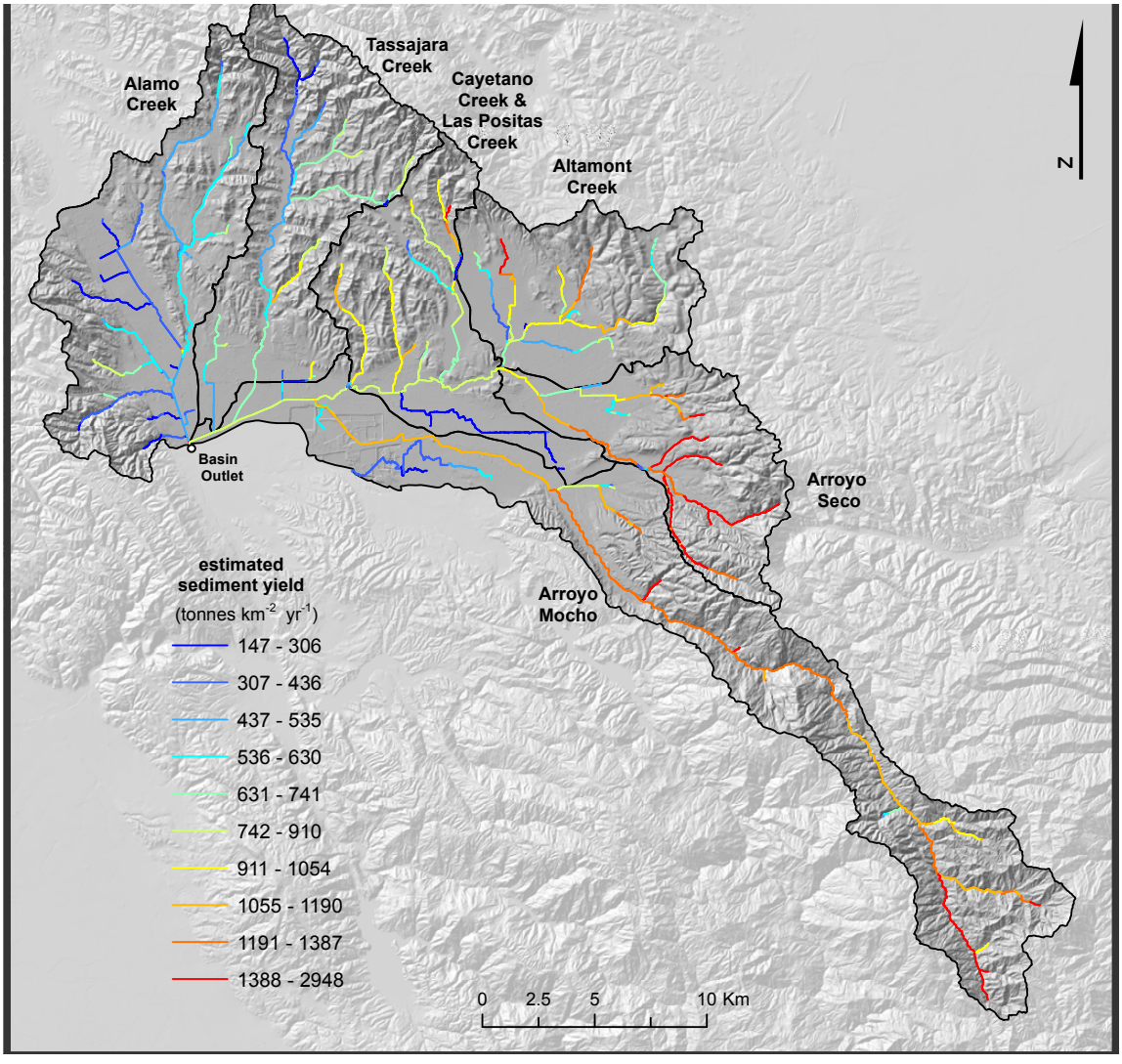

Figure 6. Estimated sediment yield aggregated downstream (summed and area weighted) through the stream network for mainstem streams (draining areas > 2 km^2).

Earth Surf. Dynam. Discuss., doi:10.5194/esurf-2016-5, 2016
Manuscript under review for journal Earth Surf. Dynam.
Published: 10 February 2016

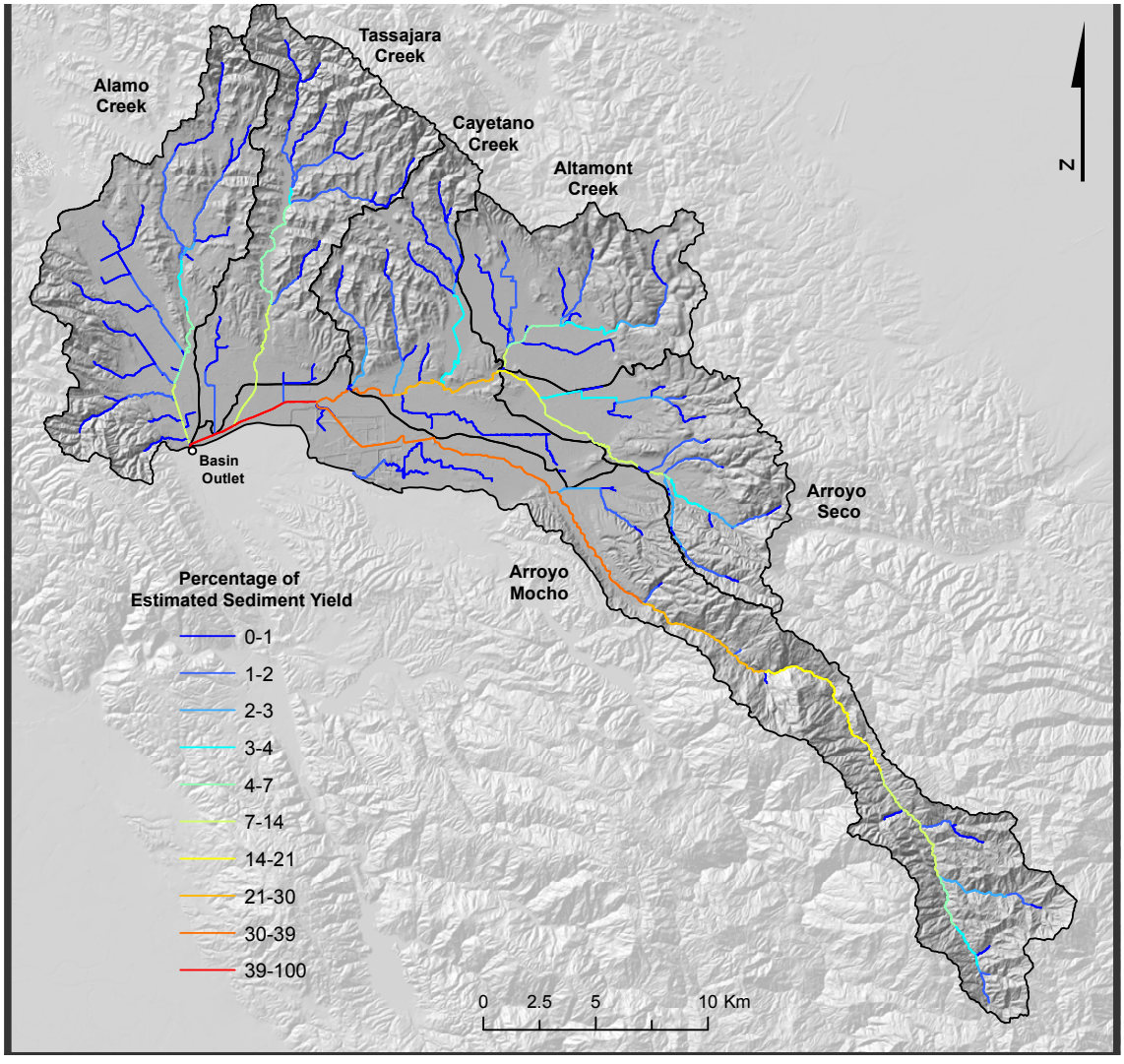

Figure 7. Percentage of total estimated sediment yield aggregated downstream through the stream network for mainstem streams (draining areas > 2 km^2).

Earth Surf. Dynam. Discuss., doi:10.5194/esurf-2016-5, 2016
Manuscript under review for journal Earth Surf. Dynam.
Published: 10 February 2016

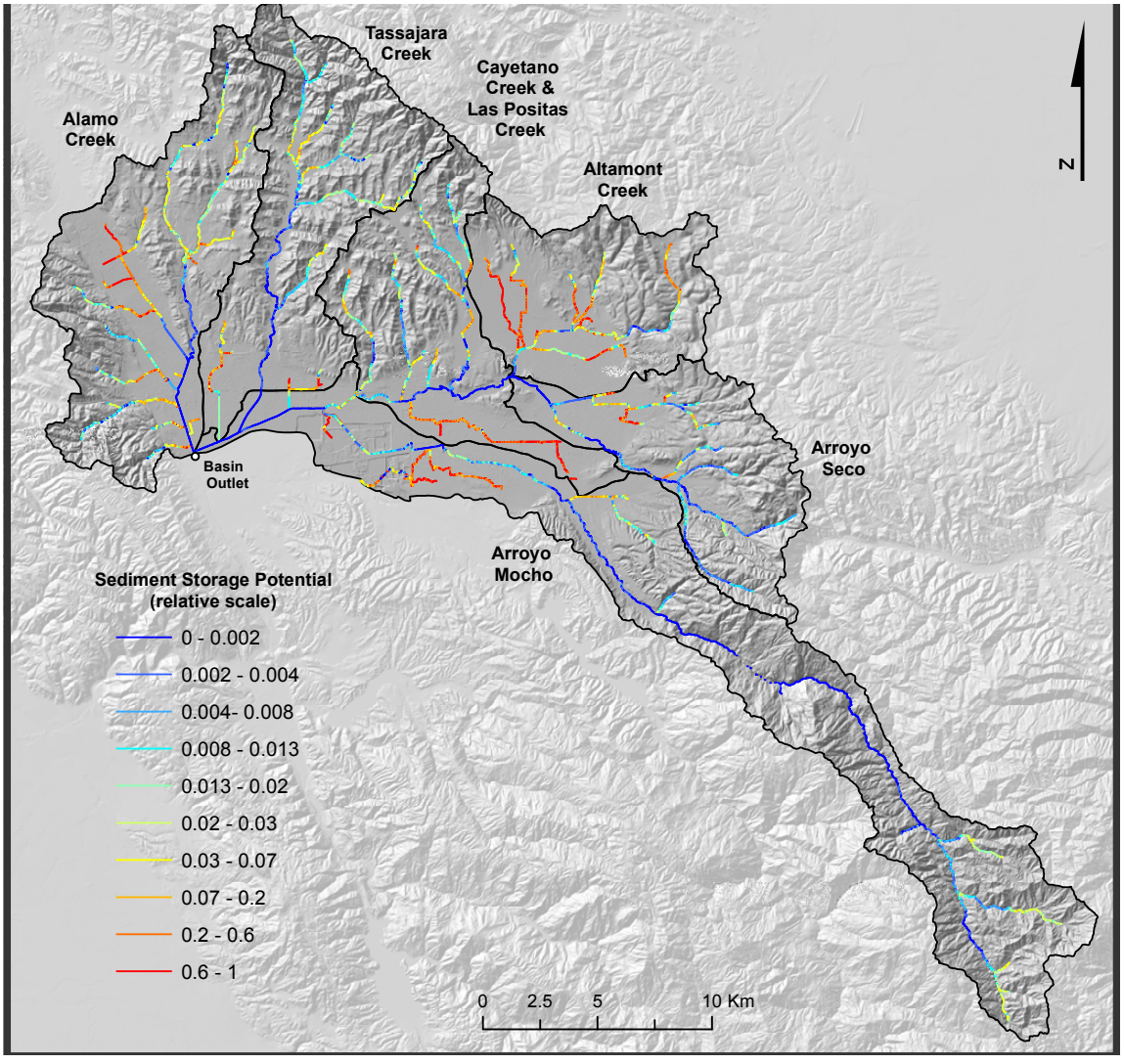

Figure 8. Estimated relative sediment storage potential for mainstem channels (draining areas > 2 km^2) based on valley width index and stream power (see text).